



## The Comparative Investigations of Structural and Optical Properties of GaSb nanocrystals / Si layers

M.V. Greben<sup>1,\*</sup>, F.F. Komarov<sup>1,†</sup>, L.A. Vlasukova<sup>1</sup>, O.V. Milchanin<sup>1</sup>, A.V. Mudryi<sup>2</sup>, I.N. Parkhomenko<sup>1</sup>

<sup>1</sup> *Belarusian State University, 4, Nezavisimosti Ave., 220030 Minsk, Belarus*

<sup>2</sup> *Scientific and Practical Materials Research Center, National Academy of Sciences of Belarus, 17, P. Brovki Str., 220072 Minsk, Belarus*

(Received 29 May 2013; published online 31 August 2013)

Optical and structural properties of GaSb nanocrystals fabricated by co-implantation of Ga and Sb ions in single crystalline Si (100), followed by thermal treatment are investigated. In the first group of samples named Si / GaSb the implantation of Ga ions was followed by Sb implantation, whereas in the second group of samples named Si / SbGa with increased by factor 1.4 ion fluence the order of implantation was inverted. The presence of nanocrystals in both kinds of samples was proved by TEM and RS experiments. Low-temperature PL measurements show a PL broad band in the region at 0.75-1.1 eV for Si / SbGa samples annealed at 900 °C. No PL was observed in the Si/SbGa samples after annealing at 1100 °C.

**Keywords:** Crystalline silicon, GaSb nanocrystals, High-fluence implantation, Broad band emission.

PACS numbers: 78.66. – w, 78.60.Fi

### 1. INTRODUCTION

Silicon has been the mainstay of the electronics industry for more than 40 years. Nowadays, CMOS at the 45 nm node being in production for a couple of years has been replaced by 32 nm and soon CMOS at the 22 nm node is expected to be in production. However, parasitic effects in current metallic interconnection have gradually become a main obstacle for further improvements with the miniaturization of devices. Therefore, the integration of microelectronic and optical circuits on one chip is highly desirable.

One of the possible implementation is to create Si-based nanostructure that contains compound semiconductor quantum dots (QDs) embedded in Si [1, 2]. The integration of  $A^3B^5$  QDs in Si is of special interest because of the near-infrared (IR) band emission in the range of 0.75-1.1 eV in PL spectra of such structures [3, 4]. It is known that this spectral range falls in one of the Si apparent windows. Recently it has been reported [5] on the formation of GaSb / Si QDs in Si by solid-source molecular beam epitaxy (MBE) on an SOI substrate. Besides the high efficient luminescence, GaSb-Si QDs demonstrates amplified spontaneous emission (ASE) in a single chip.

In this paper we report on the direct formation of GaSb nanocrystals in crystalline silicon by ion implantation followed by thermal treatment. The advantage of ion implantation technique is the area and depth selectivity of phase formation in a substrate as well as its compatibility with industrial device production lines. Thus, by focusing an ion beam or by using a suitable mask it is possible to choose the area in 2 dimensions of the nanophase nucleation. 3D control could be performed by additionally tuning the ion energy. The basic principle of this technology is built on non-equilibrium process where multiple phases can form. High fluence ion implantation produces a supersaturation of impuri-

ty species in the near surface Si layer. Subsequent thermal processing at elevated temperatures results in impurity precipitates formation within the host. Unfortunately, heavily ion irradiation results in a significant damage of Si crystalline lattice as well. "Secondary" defect formation (dislocations, microtwins) takes place even after high temperature treatment. Thus, on the one hand complex defect structures are formed during implantation and annealing, which modify numerous physical and mechanical properties of a crystal. On the other hand, the existence of precipitates has also a strong effect on the periodic order in a crystalline structure after the post-implantation annealing. The aim of this work is to present our results on structural and optical characterization of "Si + GaSb nanocrystals" system and discuss the effect of structural properties on efficiency and spectral peculiarities of photoluminescence.

### 2. EXPERIMENTAL

The specimens used for this study were prepared from lightly doped single crystalline *n*-type (100) silicon wafers with a resistivity of 4.5 Ω/cm. Two kinds of samples were prepared differed in sequence of ion implantation and fluencies. Samples of the first kind (identified as Si / GaSb) were implanted at 500 °C sequentially with Ga (250 keV) and then Sb (350 keV) ions with fluence  $D = 3.5 \times 10^{16} \text{ cm}^{-2}$  for both ion species. The samples were stored in a chamber with constant temperature  $T = 500 \text{ °C}$  between implantation of different ions. Afterwards, the samples were annealed at 1100 °C for 3, 30 and 60 min in Ar ambient. In the second kind of samples (referred to as Si / SbGa) the order of implantation ( $T_{imp} = 500 \text{ °C}$ ) of the two ion species was inverted and fluence was increased nearly by a factor 1.4 to  $D = 5 \times 10^{16} \text{ cm}^{-2}$  for both ion species. The samples were cooled to room temperature between im-

\* [leibnits@gmail.com](mailto:leibnits@gmail.com)

† [komarovF@bsu.by](mailto:komarovF@bsu.by)

plantation of different ions. After that, the samples were annealed at 900 °C or 1100 °C for 30 s-60 min in Ar ambient. The distribution of the implanted ions was simulated by Monte-Carlo method using SRIM code to obtain maximum impurity concentration at a depth of  $\sim 160$  nm from the sample surface.

The structural properties of the samples were investigated using Rutherford backscattering (RBS) and transmission electron microscopy (TEM) and diffraction (TED). The RBS spectra were collected with a collimated 1.3-1.5 MeV He<sup>+</sup> beam at a backscattering angle of 170°. We have recorded RBS spectra at two different angles of incidence of He<sup>+</sup> ions onto the sample (0° and 50°) to improve result accuracy using one detector instead of multiply detectors. TEM experiment was performed in plan-view geometry using a Hitachi H-800 instrument operating at 200 keV. The optical properties of samples were investigated by  $\mu$ -Raman spectroscopy (RS) and low temperature photoluminescence (PL) spectroscopy. RS spectra were recorded at room temperature in the backscattering geometry in the range from 90-600 cm<sup>-1</sup> using a RAMANOR U-1000 dispersive spectrometer and 532 nm YAG laser. The PL spectra were recorded in the spectral region of 0.7-2 eV using 600 nm grating monochromator in combination with a cooled to liquid nitrogen temperature InGaAs detector. During measurements the samples were immersed in a liquid helium cryostat and the 514.5 nm line of an argon ion laser was used to excite PL.

### 3. RESULTS AND DISCUSSION

Typical depth profiles of Ga and Sb atoms for the as-implanted samples which were calculated from the RBS spectra are shown in Fig. 1a. For comparison Fig. 1b depicts the ion distributions for two types of samples simulated with the computer code SRIM. One can see that simulation results represented by Pearson IV distributions.

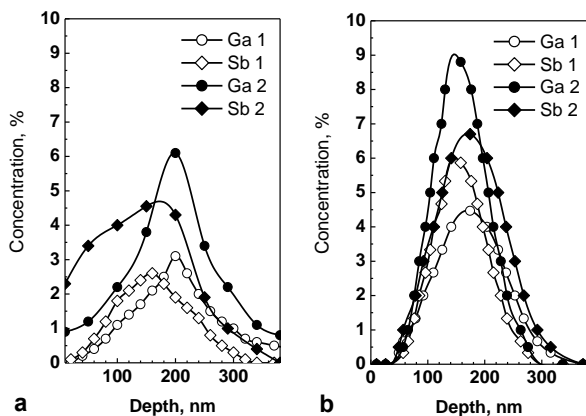


**Fig. 1** – Depth distribution of impurities in the Si / GaSb (1) and Si / SbGa (2) samples: (a) calculated from the RBS spectra depth profiles and (b) simulated with SRIM 2003

These calculations do not take into account the implantation temperature. Therefore, the simulated results are close to experimental depth profiles of implanted species for room temperature implantation [6] only. The depth profiles (Fig. 1a) were calculated from RBS spectra by fitting of the spectra using HEAD code until the simulated spectra coincided completely with the experi-

mental spectra. From Fig. 1a one can see that implantation at 500 °C already leads to a strong broadening and significant reduction of the impurity concentration as compared to the SRIM calculations that could be explained by transient enhanced diffusion (TED). This effect is weaker for Ga than for Sb. The Sb depth profiles show an asymmetric broadening towards the surface of the sample that is more obvious in the case of Si / SbGa samples. From comparison of squares under curves of simulated and calculated depth distributions of impurities we can calculate the total loss of corresponding impurity during implantation. The calculations for measured spectra show that total impurity loss is clearly less in the case of higher fluence implantation (Si / SbGa samples) in comparison with implantation of Si / GaSb samples.

In addition, the TEM measurements have been performed on both Si / GaSb and Si / SbGa samples (see Fig. 2).

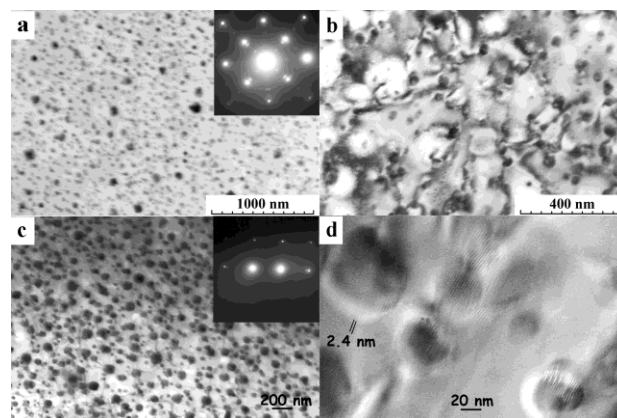


**Fig. 2** – TEM of implanted samples after the annealing at 1100 °C for 30 min (a-b) and 60 min (c-d). (a) Si / GaSb sample; (b) Si / SbGa sample

The micrographs showed the presence of faceted GaSb nanoprecipitates for all types of samples. The crystalline nature of the precipitates is proved by the presence of Moire fringe patterns in the TEM images (Fig. 2d). One can see small extra reflexes besides basic Si matrix reflexes at electron diffraction pattern (insert in Fig. 2a). These extra reflexes location is similar to the location of twin Si reflexes. As we failed to register aligned RBS spectra in as-implanted or annealed samples we can state that subsurface Si layer even after long time annealing at 1100 °C are heavily damaged and is near amorphous state. At the same time the Si matrix is still crystalline because of the registered a narrow peak at 512 cm<sup>-1</sup> in Raman spectra (not shown) of annealed samples that corresponds to zone-center phonons scattering of crystalline silicon. It should be noted that a significant shift towards low frequencies occurs in comparison with the peak's position at 521 cm<sup>-1</sup> of undamaged Si [7]. This shift is caused by the presence of significant mechanical strains within the implanted layer. Raman spectra of each type of as-implanted samples did not reveal any peak corresponding to crystalline GaSb (see Fig. 3b). However, in the spectra of both Si / GaSb and Si / SbGa annealed samples a peak at 235-237 cm<sup>-1</sup> is observed. We attribute this peak to LO-phonon scattering of crystalline GaSb [8]. Besides it two additional peaks at 112 and

150  $\text{cm}^{-1}$  are dominated in RS spectra (see Fig. 3). We attribute them to LO- and TO-phonon scattering of crystalline Sb. Thus, the thermal processing of the samples with high Sb and Ga concentrations leads to the formation of both GaSb and Sb precipitates within the Si matrix. A similar situation was reported by other authors for Si implanted at 500 °C with high fluence of As and In ions [4]. After annealing both InAs and crystalline In precipitates were detected by X-ray diffraction.

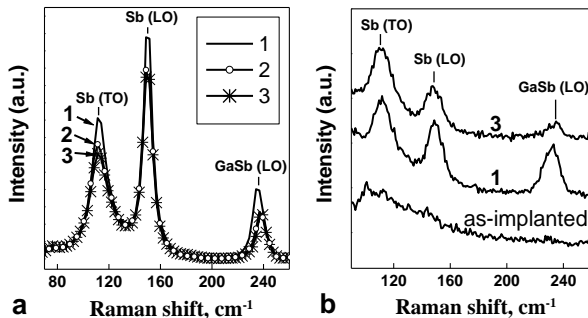


**Fig. 3** – Raman spectra of implanted samples after the annealing at 1100 °C for 3 (1), 30 (2) and 60 (3) min. (a) Si / GaSb sample; (b) Si / SbGa sample

In Fig. 4 low-temperature PL spectra of the two kinds of samples are depicted.

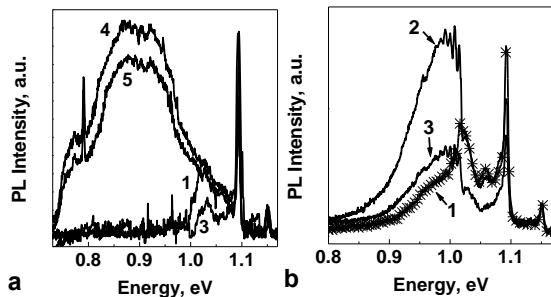


**Fig. 4** – PL spectra of Si samples after the annealing at 900 °C for 30 s (4) and 45 min (5) and at 1100 °C for 3 (1), 30 (2) and 60 (3) min. (a) Si / SbGa sample; (b) Si / GaSb sample

The sharp lines at 1.09 eV and 1.15 eV are related to

bound exciton phonon-less and phonon assisted recombination at main residual doping impurity (Phosphorus) or implanted donor impurity (Antimony). Besides them, a broad band with a maximum at 0.9 eV dominates in the PL spectrum of the annealed at 900 °C Si / SbGa samples (see Fig. 4 a). A similar band was observed earlier in the PL spectra of silicon samples with embedded tin ( $\alpha$ -Sn) QDs in the work [9]. Sn QDs were formed in Si (100) as result of heat treatment up to 800 °C of a few nanometer thick  $\text{Sn}_x\text{Si}_{1-x}$  layers with  $x \leq 0.1$  grown on Si surface. The appearance of this broad band was attributed to the presence of defects introduced by the grown layers. In the experiment under consideration here, the similar band is registered in PL spectra of Si implanted with Sb and Ga ions. Thus, the question about the nature of this band arises. There are at least three possible explanations of near-IR photoluminescence origin for “Si + SbGa nanocrystals”. They are: carrier recombination inside GaSb NCs, radiative recombination at the nanocrystal / Si matrix interfaces and dislocation-related luminescence. After the annealing at 1100 °C the band at 0.75-1.1 eV disappears in the PL spectra (see Fig. 4a). At the same time the PL spectra of Si / GaSb samples annealed at 1100 °C exhibit a series of relatively sharp lines at successive line spacing of 8 meV (see Fig. 4b). The spectrum transformations could be related to annealing of a part of dislocation-type defects and is presently under study by our team.

#### 4. CONCLUSIONS

The comparisons of structural and optical properties of 2 kinds of samples are presented. A significant impurity loss of both implanted species in Si / GaSb samples has been revealed as a result of “hot” implantation conditions. The formation of GaSb nanocrystals have been registered in all annealed at 900-1100 °C samples using TEM and RS experiments. It has been shown that nanocrystals are formed in the near-surface 300 nm heavily damaged layer containing a lot of defects. A broad line at 0.75-1.1 eV is found in the low-temperature PL spectra of Si / SbGa samples annealed at 900 °C for 30 s-45 min. Annealing of Si / SbGa samples at 1100 °C for 3-60 min results in disappearing of the BB in PL spectra.

#### REFERENCES

1. S. Prucnal, S. Zhou, X. Ou, H. Reuther, M.O. Liedke, A. Mucklich, M. Helm, J. Zuk, M. Turek, K. Puzniak, W. Skorupa, *Nanotechnology* **23**, 1 (2012).
2. Y.K. Huang, C.P. Liu, Y.L. Lai, C.Y. Wang, Y.F. Lai, H.C. Chung, *Appl. Phys. Lett.* **91**, 091921 (2007).
3. F. Komarov, L. Vlasukova, W. Wesch, A. Komarov, O. Milchanin, S. Grechnyi, A. Mudryi, A. Ivankovich, *Nucl. Instrum. Meth. B* **266**, 3557 (2008).
4. A.L. Tchebotareva, J.L. Brebner, S. Roorda, C.W. White, *Nucl. Instrum. Meth. B* **175-177**, 187 (2001).
5. N. Yasuhara, M. Jo, Y. Sugawara, K. Kawamoto, S. Fukatsu, *J. Cryst. Growth* **301-302**, 718 (2007).
6. F.F. Komarov, O.V. Milchanin, L.A. Vlasukova, W. Wesch, A.F. Komarov, A.V. Mudryi, *B. Russ. Acad. Sci. Phys.* **74**, 252 (2010).
7. F. Komarov, L. Vlasukova, O. Milchanin, A. Mudryi, B. Dunets, W. Wesch, E. Wendler, *phys. status solidi a* **209**, 148 (2012).
8. M. Landolt, J. Bornstein, *Numerical data and functional relationships in science and technology, New series* (Springer-Verlag: Berlin-Heidelberg: 1982).
9. A. Karim, G.V. Hansson, W.X. Ni, P.O. Holtz, M. Larsson, H.A. Atwater, *Opt. Mater.* **27**, 836 (2005).